Low-Cost and High-Volume Production of Lightweight Engineered Cellular Materials

Jordan Cioni

Physics; University of Wisconsin-River Falls, River Falls

Abstract

Production of C954 Aluminum-Bronze cellular material specimens is attempted by employing a lost-wax casting processes. Double Gyroid casting patterns are created using a consumer grade FDM printer equipped with wax filament. The high temperature sensitivity of wax filament is found to inhibit the creation of high precision models. Furthermore, misrun defects reveal that a high-temperature furnace alone is insufficient to cast materials with high liquidous temperatures. Recommendations are made to improve the process of high-precision investment casting with high melting point alloys and low-cost, consumer grade equipment.

Introduction

Materials that are simultaneously lightweight, strong, and shock absorbing are needed in all areas of the built environment. Developments in earthquake-prone areas must have foundations that support a building while withstanding tremendous vibrations. Football helmets must gently absorb impacts to prevent concussions yet they must also be strong enough to prevent blunt force trauma and be light enough to wear. Armored vehicle frames must not fail in the face of rough terrain or collisions, yet they must also readily dissipate mechanical energy the in event of high velocity impacts without while maintaining an efficient weight. In the design of shock absorbing products, a historic challenge is presented by the tradeoff between material strength and damping characteristics. Traditional materials used in shock absorbing applications such as foams and rubbers lack the strength required of load bearing members. At the same time, materials used in load bearing applications often transmit vibrations with insufficient damping capabilities for a shock absorbing application.

When designing lightweight mechanical systems that must withstand impact loading, one common approach is the incorporation of cellular materials such as foam and wood. Cellular materials are classified as assemblies of struts or plates, filling space and forming the edges and faces of cells [8]. These materials allow for selective optimization of strength, mechanical energy absorption, and mass [4]. Because of their novel mechanical characteristics and intrinsic light-weight nature, cellular materials commonly play energy absorbing applications in automotive, aerospace, and biomedical applications [13] [1] [15] [14]. However, by implementing conventional cellular materials, shock-damping behaviors and efficient weights are obtained at the cost of overall strength. Furthermore, traditional cellular material production processes (bulk foaming and strut assembly [10]) lack sufficient control to yield consistent material properties [7].

Following the advent of additive manufacturing (AM), precise design and production of cellular materials lead to a new classification of materials: engineered cellular materials. Thereafter, academic and industrial researchers have devoted extensive research efforts to the characterization of engineered cellular materials. Bai et al. (2020) showed that lattice structures with non-uniform density gradients possess superior strength and energy absorbance compared to structures with uniform density [5]. Structures exhibiting stretching-dominated deformation were shown to

This material is based upon work supported by NASA under Award No. UGR23_3-0 issued through the Wisconsin Space Grant Consortium. Any opinions, findings, and conclusions or recommendations expressed in this material are those of the author(s) and do not necessarily reflect the views of the National Aeronautics and Space Administration.

possess greater specific strength than bending-dominated structures by Deshpande et al. (2001) [6]; while Li et al. (2019) revealed that bending-dominated structures possess superior energy absorption capabilities compared to stretching-dominated structures [10]. Khaderi et al. (2014) found that, in comparison to lattice-based structures, topological optimization yields superior specific properties. This also revealed that cellular materials offer superior specific properties in situations with unknown loading conditions [5].

In high-tech transportation industries, the high specific strength of cellular materials provides a simple means of reducing a vehicle's overall mass without compromising its strength. But despite significant research of novel high-strength cellular materials, manufacturing firms are unable to implement cutting-edge cellular materials because of the high production costs associated with directed laser metal sintering (DLMS), the traditional method of producing engineered cellular materials. In addition to overhead costs, DLMS prototype production is a time consuming process which places significant restrictions on material options and overall part size.

In this project, the primary goal is to demonstrate that lost-wax casting, or investment casting, is an effective alternative to DLMS production of engineered cellular materials. The lost-wax casting process is a well-known casting technique widely applied in the jewelry and dental industries because of its ability to preserve fine details. Compared to the DLMS process, the traditional method of producing engineered cellular materials, the lost-wax process offers significant benefits in the key areas of production volume, cost, and strength.

Materials and Methods

A well-studied variation of the Schoen Gyroid, referred to as the "Double Gyroid," is selected as the engineered cellular material geometry to be cast. Discovered by A. Schoen (1970), the Schoen Gyroid is a triply periodic minimal surface defined by Eq. 1 of (Shoen, 1970) that exhibits high stiffness and a low maximum Von Mises stress [2]. Among gyroid permutations, the Double Gyroid is known to possess superior mechanical properties [1]. Under hydrostatic loading, gyroid solids display stretching dominated behavior, while all other loading induces bending dominated deformations [9]. In Fig. 1, an isosurface plot illustrates the double gyroid surface.

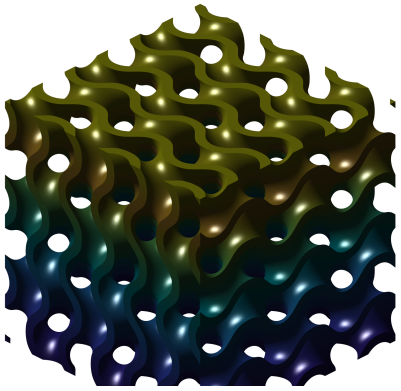

Figure 1: Isosurface plot of nine cubically of Double Gyroid unit cells with isovalue of 0.55.

To conduct the investment casting, wax patterns of material specimen and gating system are required. Using MATLAB, 1 inch cubes consisting of nine cubically arranged gyroid unit cells are triangulated and converted into .stl files. OnShape is used to model the gating system, shown in Fig. 2, which consists of a one-piece sprue, runner, and gate. A typical gating system consists of a central, cylindrically-shaped sprue with narrow runners branching off towards the gates that interface with the desired part. Because the thin walls of the gyroid are expected to rapidly solidify, the runners are omitted

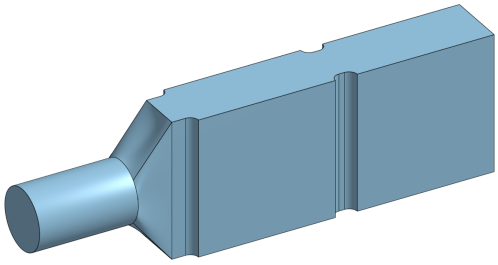

Figure 2: OnShape model of gating system with rectangular sprue and four 1 inch gates to allow for simultaneous casting of multiple cellular material specimens.

to minimize thermal losses as molten metal flows from the sprue which acts as a reservoir. Additionally, the sprue is designed with a rectangular profile instead of cylindrical to enable faster and more reliable pattern creation using a consumer grade Fused Deposition Modelling (FDM) 3-D printer.

The casting patterns are created using an Ender 3 Pro FDM printer equipped with a standard 0.4 mm nozzle. Patterns are made with Castable Wax filament printed at 30 m/s with a nozzle temperature of 135 °C. To improve printing quality and speed, the cellular material specimens and gating systems are printed separately. After printing, the material specimen is bonded to the gating system using molten wax.

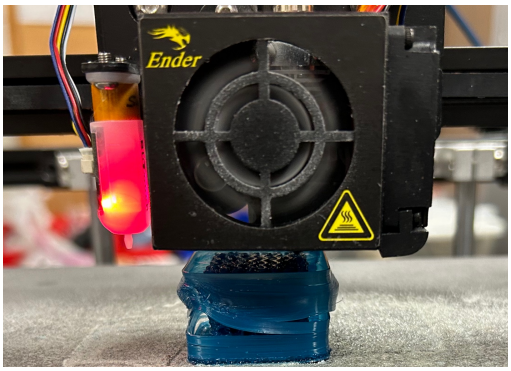

Figure 3: Cellular material pattern printing on an Ender 5 Pro equipped with a 0.4mm nozzle. Surrounding the pattern, a thin wall is printed to contain warm air and allow for slower cooling of printed material.

To prepare the casting mold, the wax patterns are fixed in a 316 stainless steel casting flask and surrounded by a gypsum bonded investment slurry with an investment to water ratio of 2:1. Prior to solidification, the flask is placed in a sealed container and air is evacuated using a canister vacuum to remove trapped pockets of gasses from the slurry. After one minute of low-vacuum exposure, the casting flask is removed and allowed to solidify. The mold is then placed in a Vcella 9 kiln and the investment material's recommended burnout cycle is performed to completely remove wax material without damaging the hollow, pattern-shaped cavity. Once the burnout process is complete, the hardened mold is held in a secondary oven at 275 °C to mitigate thermal shocks and cooling-induced misruns when molten metal is introduced.

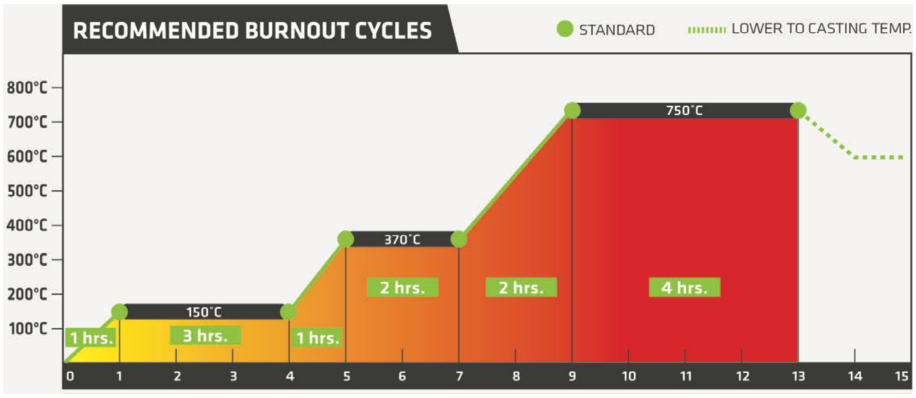

Figure 4: Temperature-time curve depicting the recommended wax burnout cycle for Prestige Oro investment power [11].

The total volume of the gyroid patterns and gating system is evaluated and the corresponding length C954 Aluminum-Bronze stock is placed in a graphite crucible in the Vcella furnace at 1150 °C. This temperate, which exceeds the alloy's liquidous temperature of 1040 °C [3], is selected to ensure a complete phase change and lower the molten alloy's viscosity while remaining below the furnace's maximum operating temperature of 1260 °C. Depending on the total volume of material, the casting process is ready to proceed after a period of four to six hours.

To begin the casting process, the mold is removed from the secondary furnace and placed in a fume hood to prevent inhalation of metal vapors during metal pouring and solidification. Immediately after the mold is placed, the crucible of molten metal is removed from the furnace and rapidly poured into the mold before cooling of the mold or metal induces premature solidification. The metal is allowed to cool with the fume hood completely closed. Before reaching room temperature, the cast part is devested by quenching in room temperature water. Large pieces of investment material that remain on the part are removed using a low-pressure water jet, and fine pieces are removed using an ultrasonic bath.

Figure 5: Immediately after removing mold from secondary oven, the mold is placed in a fume hood to minimize exposure to metal vapors and the crucible containing molten metal is removed from the furnace (left) and carefully poured into the mold (right).

Key Results

Using a consumer grade FDM printer to produce casting patterns was found to inhibit the creation of high precision models. The high thermal sensitivity of casting wax severely restricted the range of effective printing temperatures. Nozzle temperatures exceeding 135 ^{o}C resulted in excessive stringing defects and over-extrusion. Simultaneously, temperatures at or below 130 ^{o}C failed to promote consistent layer adhesion. Furthermore, when printing at slow speeds to encourage low temperature layer adhesion while avoiding high temperature defects, prolonged exposure to ambient air and heat radiating from the printhead resulted in significant model warping.

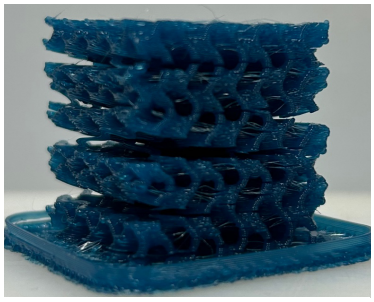

Figure 6: Wax pattern printed with 130 ^{o}C nozzle temperature and 10 mm/s layer speed shows sever warping induced layer separation.

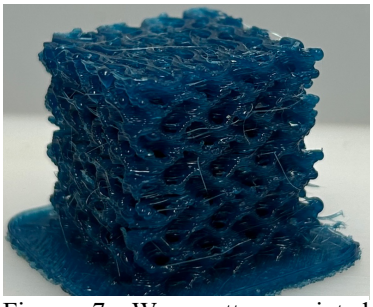

Figure 7: Wax pattern printed using nozzle temperature of 135 ^{o}C exhibits stringing and large blobs that result from over extrusions.

When casting molten metal into low-temperature molds, repeated misruns were observed that are assumed to prevent molten material from penetrating thin-walled features of cellular material patterns. The first casting attempt, shown in Fig. 8, was performed with a room temperature mold which resulted in minimal penetration into the cellular material cavity. In later attempts, 275 °C mold temperatures achieved using an oven slightly prolonged solidification times, which allowed for improved penetration of the cellular material cavity; however, this mold temperature still subjects molten material to a sudden temperature change of 875 °C. As such, cooling-induced misruns are still observed.

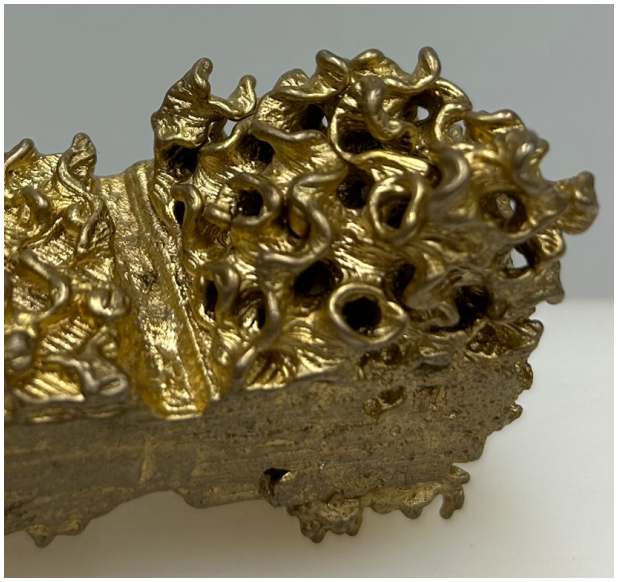

Figure 8: Using additional ventilation and a mold temperature of 275 °C, significantly improved penetration on thin features is observed; however, premature solidification continues to induce misrun defects.

Figure 9: The first casting attempt, performed with a room temperature mold, subjected molten material to a rapid temperature change of 1015 °C. Minimal material penetration is observed in the walled cellular material cavities.

Discussion

In the current phase of this project, results indicate the originally proposed methodology must be refined in order to produce low-cost engineered cellular materials that are comparable to those obtained by DLMS manufacturing. It is well-demonstrated that FDM printing is an inadvisable means of producing temperature-sensitive wax patterns. To circumvent the thermal challenges posed by FDM printing it is recommended that stereolithography (SLA) 3D printers equipped with wax resin be considered as an alternative pattern production tool. Using consumer grade SLA printers, geometric resolution at the micrometer scale is achievable without significant overhead costs.

In addition, cooling-induced misruns must be addressed in order to obtain functional cast cellular materials. To reduce the rapid cooling caused by low mold temperatures, potential solutions include heating of the mold in the melting furnace, a secondary furnace, or with a bunsen burner. To maximize solidification time, the mold should ideally be held at the same temperature as the molten metal. This can be achieved by heating the mold in the melting furnace; however, typical casting flasks made of 316 stainless steel will begin to anneal at 1040 °C, resulting in significantly safety risks due to increased ductility. To precisely obtain a safe and effective mold temperature, an oven is insufficient. Therefore, an additional high-temperature furnace must be

implemented. In contrast, the low-cost option of an open flame burner is a promising method of achieving high temperatures but lacks the ability to provide precise and uniform heating.

As this ongoing project continues, additional casting attempts will be performed to evaluate methods of effective mold heating. Once this methodology is sufficiently improved, cellular material specimens fabricated using lost wax casting will be subjected to mechanical evaluation. Standard material characterization tests such as mass density, quasistatic loading, tensile failure testing, and torsional failure testing will be conducted to compare with the results of similar tests performed with DLMS produced gyroid samples.

Acknowledgments
Thanks to the University of Wisconsin-River Falls URSCA grant committee and WSGC for funding this work, and to Dr. Lowell McCann and Dr. Jagdeep Thota for their mentorship and encouragement.

References

[1] Aremu, A. O., Brennan-Craddock, J. P. J., Panesar, A., Ashcroft, I. A., Hague, R. J. M., Wildman, R. D., & Tuck, C. (2016). A voxel-based method of constructing and skinning conformal and functionally graded lattice structures suitable for additive manufacturing. *Additive Manufacturing, 13,* 1-13. https://doi.org/10.1016/j.addma.2016.10.006

[2] Aremu, A. O., Maskery, I., Tuck, C., Ascroft, I. A., Wildman, R. D., & Hague, R. I. M. (2014). A Comparative Finite Element Study of Cubic Unit Cells for Selective Laser Melting. *2014 International Solid Freeform Fabrication Symposium.*

[3] (August 6th, 2023). *Aluminum Bronze, UNS C95400, Copper Casting Alloy, TQ50 Temper.* MatWeb. https://www.matweb.com/search/datasheet.aspx?matguid=2e3b6e47d3224e45b9fcd5e876ab7770&ckck=1

[4] Ashby, M.F., Medalist, R.F.M. The mechanical properties of cellular solids. *Metall Mater Trans A 14***,** 1755–1769 (1983). https://doi.org/10.1007/BF02645546

[5] Bai, L., Gong, C., Chen, X., Sun, Y., Xin, L., Pu, Y., & Luo, J. (2020). Mechanical properties and energy absorption capabilities of functionally graded lattice structures: Experiments and simulations. *International Journal of Mechanical Sciences, 128,* 105735. https://doi.org/10.1016/j.ijmecsci.2020.105735

[6] Deshpande, V.S., Ashby, M.F., & Fleck, N.A. (2001). Foam topology: bending versus stretching dominated architectures. *Acta Materialia, 49,* 1035-1040. https://doi.org/10.1016/S1359-6454(00)00379-7

[7] Evans, A. G., Hutchinson, J. W., Ashby, M. F. (1998). Cellular metals. *Current Opinion in Solid State & Materials Science, 3.* 288-308.

[8] Gibson, L.J. Cellular Solids. *MRS Bulletin* 28**,** 270–274 (2003). https://doi.org/10.1557/mrs2003.79

[9] Khaderi, S. N., Deshpande, V. S., & Fleck, N. A. (2014). The stiffness and strength of the gyroid lattice. *International Journal of Solids and Structures, 51,* 3866-3877. http://dx.doi.org/10.1016/j.ijsolstr.2014.06.024

[10] Li, D.; Liao, W.; Dai, N.; Xie, Y.M. (2019). Comparison of Mechanical Properties and Energy Absorption of Sheet-Based and Strut-Based Gyroid Cellular Structures with Graded Densities. *Materials*, *12*, 2183. https://doi.org/10.3390/ma12132183

[11] Prestige investment powders. "Oro." (accessed August 6th, 2023). https://www.certus-int.com/docs/ORO.pdf

[12] Schoen, A. H. (1970). Infinite Periodic Minimal Surfaces Without Self-Intersection. *National Aeronautics and Space Administration.*

[13] Tan H., Qu S. (2010). Impact of Cellular Materials. In: Altenbach H., Öchsner A. (eds) Cellular and Porous Materials in Structures and Processes. CISM International Centre for Mechanical Sciences, vol 521. Springer, Vienna. https://doi.org/10.1007/978-3-7091-0297-8_6

[14] Yang, E., Leary, M., Lozanovski, B., Downing, D., Mazur, M., Sarker, A., Khorasani, A., Jones, A., Maconachie, T., Bateman, S., Easton, M., Qian, M., Choong, P., & Brandt, M. (2019). Effect of geometry on the mechanical properties of Ti-6Al-4V Gyroid structures fabricated via SLM: A numerical study. *Materials and Design, 184,* 108165. https://doi.org/10.1016/j.matdes.2019.108165

[15] Yang, L., Mertens, R., Ferrucci, M., Yan, C., Shi, Y., & Yang, S. (2019). Continuous graded Gyroid cellular structures fabricated by selective laser melting: Design, manufacturing and

mechanical properties. *Materials and Design, 162,* 394-404. https://doi.org/10.1016/j.matdes.2018.12.007